Role of the Major Homology Region in Assembly of HIV-1 Gag†

P. Provitera,‡ A. Goff,§ A. Harenberg,§ F. Bouamr,§ C. Carter,*,§ and S. Scarlata*,‡

Department of Physiology and Biophysics and Department of Molecular Genetics and Microbiology, State University of New York at Stony Brook, Stony Brook, New York 11794

Received August 28, 2000; Revised Manuscript Received March 1, 2001

ABSTRACT: The major homology region (MHR) is a highly conserved sequence in the *gag* gene of all retroviruses, including HIV-1. Its role in assembly is unknown, but deletion of the motif significantly impairs membrane binding and viral particle formation. To begin characterizing this defect, we have determined the contribution of this region to the energetics of the assembly process. Intrinsic fluorescence studies were conducted to determine the change in free energy associated with membrane and RNA binding using tRNA and large unilamellar vesicles of 1-palmitoyl-2-oleoylphosphatidylserine as models. For the wild-type protein, the change in free energy was within *RT* [600 cal/(mol·K)] whether Gag binds first to RNA or to the membrane. Thus, the initial binding of Gag can be to either substrate, but in vivo conditions favor initial association to RNA presumably due to its higher local concentration. After establishing the pattern of assembly, we compared the binding energy of Gag_{WT} versus the deletion mutant, $Gag_{\Delta MHR}$. Gag_{WT} bound to membranes with a 2-fold higher affinity than $Gag_{\Delta MHR}$, and the binding to RNA was similar for the two proteins. Gag prebound to RNA or to membrane exhibited ∼2−4-fold greater binding affinity than $Gag_{\Delta MHR}$ for binding the membrane or RNA, respectively. Most importantly, the mutant was significantly impaired in its ability to self-associate on RNA or on membrane surfaces. This key role of the MHR in promoting productive protein−protein interactions was also seen in altered amounts of cleavage products and the lack of membrane-bound, RNA-containing replication intermediates in infected cells. These results suggest that Gag first binds to RNA and then assembles into a multimeric complex with a large membrane-binding face that facilitates subsequent membrane binding. Deletion of the MHR disrupts the protein−protein interactions required to complete this process.

An important part of the life cycle of retroviruses, whose members include the human immunodeficiency virus (HIV),[1] involves the assembly of Gag precursor proteins and viral RNA and the plasma membrane of host cells for release by budding. Although these three components are initially in different regions of the host cell, they assemble to form the viral particle. Gag is later processed into the membrane-interacting matrix (MA) protein, capsid (CA) protein, p6, whose function may involve dissociation of virions from the host and the RNA-binding nucleocapsid (NC) protein (*1*). Whether membrane binding precedes RNA binding is not clear.

The protein domains of Gag each play different roles in the life cycle of the virus. During assembly of the virus in host cells, the N-terminal MA domain of Gag targets the protein to the plasma membrane and serves to incorporate the membrane-spanning envelope proteins into the newly forming virion (*2*, *3*). After entry of the virus into cells, a population of MA dissociates from the membrane to expose a nuclear localization sequence, which allows the transport of viral proteins into the nucleus enabling HIV-1 to replicate in nondividing cells (*4*). The C-terminal NC domain contains two copies of the highly conserved cysteine-histidine motif and is influential in recognition and incorporation of viral RNA into the particle (*5*−*7*). Located in the center of the Gag sequence is the CA domain, whose role in the viral life cycle is less understood. Evidence exists for its essential role in particle assembly (*8*, *9*) and packaging of the cellular host protein cyclophilin A (*10*, *11*). However, how these events occur remains to be elucidated. Morphologically, mature CA forms the distinctive conical core of the virus that encapsulates the viral RNA−protein complex. Other than providing structural stability of the virion, the function of CA is largely unknown.

Within the CA portion of Gag there is a highly conserved region of amino acids known as the major homology region (MHR). This region is conserved throughout the retrovirus group (*8*) and thus offers a novel and stable target for viral vaccines. The role of the MHR region has been investigated using mutagenesis strategies. Various mutations within the MHR block viral replication at different and distinct stages, such as assembly, maturation, and infectivity (*12*−*14*), indicating that MHR may play a role in Gag interactions with the host membrane and/or with viral RNA. Direct evidence that MHR plays a role in membrane binding comes

† This work was supported by National Institutes of Health Grant GM58271.

* To whom correspondence should be addressed. S.S.: e-mail, suzanne@dualphy.pnb.sunysb.edu; telephone, (631) 444-3071. C.C.: e-mail, ccarter@ms.cc.sunysb.edu; telephone, (631) 632-8801.

‡ Department of Physiology and Biophysics.

§ Department of Molecular Genetics and Microbiology.

[1] Abbreviations: HIV-1, human immunodeficiency virus type 1; MA, matrix; CA, capsid; NC, nucleocapsid; coumarin, 7-(diethylamino)-3-(4′-maleimidylphenyl)-4-methylcoumarin; dabsyl, 4-[[4-[[4-(dimethylamino)phenyl]azo]phenyl]azo]benzoic acid succinimdyl ester; POPS, 1-palmitoyl-2-oleoylphosphatidylserine; LUVS, large unilamellar vesicles.

10.1021/bi002040l CCC: $20.00
Published on Web 04/11/2001

from biophysical studies showing that purified MHR-deleted Gag has a reduced affinity to model membranes as compared to wild type (*15*). These results suggest that the MHR mediates the Gag conformation required for productive protein−protein and protein−membrane interactions during assembly.

Since the MHR of HIV is so highly conserved, it is an attractive target for drug design. Knowing which step in assembly is regulated by the MHR may offer direction in the development of therapeutic agents. Here, we have first defined the assembly sequence of Gag onto membranes and RNA by determining the energetics of these associations and by determining the amounts of intermediates formed in virally infected cells. We then directly compared the free energy accompanying the binding of Gag_{WT} and an MHR deletion mutant ($Gag_{\Delta MHR}$) to model membranes and tRNA and the energy associated with the protein assembly of Gag bound to either of these two surfaces. Our results lead to the conclusion that Gag_{WT} follows the following assembly sequence: Gag first binds to RNA where it then undergoes oligomerization and, after, the complex binds to the plasma membrane. We find that while MHR plays only a minor role in directing the binding of Gag membranes or RNA, it plays a critical role in mediating productive protein assembly of Gag bound to either of these substrates.

MATERIALS AND METHODS

Sample Preparation. The wild-type and mutated recombinant HIV-1 Gag proteins used in this study were prepared as previously described (*15*). Large unilamellar vesicles (LUVS, 0.1 mm diameter) composed of 1-palmitoyl-2-oleoylphosphatidylserine (POPS) were prepared by extrusion. The buffer used for these studies was composed of 0.5 M NaCl, 40 mM HEPES, and 1 mM DTT unless noted otherwise.

HIV-1 Gag was labeled with fluorescein-5-isothiocyanate (FITC) by addition of the probe from a concentrated stock in dry DMSO at a 3:1 probe:protein molar ratio. The solution was allowed to react overnight at 5 °C, and unreacted probe was removed by dialysis against 40 mM Hepes (pH 7.0), 0.5 M NaCl, and 1 mM DTT. The labeling ratio, as determined by comparing the probe concentration measured by absorption to the protein concentration measured by a Bradford dye binding assay (Bio-Rad), was found to be 1:1 for both wild-type and ΔMHR Gags. HIV-1 Gag was labeled with coumarin succinyl ester or dabsyl succinyl ester by first raising the pH to 8.5, adding a 4-fold molar excess of the probe from a concentrated DMF stock, incubating on ice for 20 min, and then extensively dialyzing the sample overnight in buffer. Labeling of Gag with either of these probes had no significant effect on membrane binding (see ref *16*) or tRNA binding (Provitera et al., unpublished results).

Fluorescence Titrations. All fluorescence measurements were made using an ISS fluorometer (I.S.S., Inc., Champaign, IL) with samples contained in microcuvettes with a path length of 3 mm.

Fluorescence heterotransfer was measured by covalently labeling one set of proteins with the fluorescence resonance energy donor, coumarin succinyl ester, and a second set with the energy transfer acceptor, dabsyl SE. Heterotransfer was measured by monitoring the ∼30% loss in emission intensity of coumarin−Gag as its fluorescence is transferred to the nonfluorescent dabsyl−Gag acceptor. These studies were carried out by starting with 10 nM coumarin−Gag in buffer, incrementally adding dabsyl−Gag, and integrating the coumarin spectra from 380 to 440 nm; $\lambda_{ex} = 360$ nm. Control studies substituted either buffer for the dabsyl−Gag. Control studies substituting unlabeled protein gave identical results.

Fluorescence homotransfer was measured by monitoring the anisotropy of FITC−HIV-1 Gag at $\lambda_{ex} = 490$ nm and $\lambda_{em} = 516$ nm and correcting for background scattering due to lipid or tRNA at the identical buffer conditions. Measurements were made by starting at 0 nM protein and adding small amounts of protein until 200 nM was reached.

Membrane and RNA binding assays using intrinsic fluorescence were conducted using 200 nM HIV-1 Gag protein and adding small amounts of tRNA from an 800 μM stock and freshly extruded 2 mM POPS LUVs. Changes in the intrinsic fluorescence were monitored by recording the spectra using $\lambda_{ex} = 280$ nm, scanning from 320−400 nm, and calculating the integrated intensity. Because binding of HIV-1 Gag protein is very strong, low concentrations of lipids and tRNA could be used. The contribution of scattered light never exceeded more than 1% of the total intensity. Control studies were done to ensure that the addition of buffer alone did not affect protein emission.

Reversibility of membrane binding was carried out by binding 100 nM Gag to 10 μM POPS bilayers doped with 2% dansyl−PE (Molecular Probes, Inc.), which results in a 10% increase in dansyl emission and following the reversal of this increase when a 50-fold excess of unlabeled POPS is added. Reversibility of tRNA binding was measured by binding fluorescein-labeled Gag to the RNA, which reduces the fluorescein emission and following the reversal of this decrease when a 50 excess of unlabeled Gag was added.

Changes are reported on the basis of changes in the normalized emission energy:

$$\text{normalized emission energy} = (CM_i - CM_x)/CM_f$$

where the subscripts i, x, and f denote the initial, intermediate, and final concentrations of HIV-1 Gag. CM is the center of the spectral mass calculated from the emission energy [EE; units of energy given in kilokaisers (kK), where 1 kK = 1000 cm^{-1}] and intensity (INT) at each wavelength (i):

$$CM = \sum_i (EE)_i (INT)_i / \sum_i (INT)_i$$

Binding of substrate-bound Gag to the second ligand was carried out using intrinsic fluorescence. These binding studies were accomplished by titrating the substrate (POPS or tRNA) into 200 nM protein in buffer or into 200 nM protein with either 40 or 83 μM POPS, or to 16 or 33 μM tRNA, and scanning the emission from 320 to 400 nm using an exciting wavelength of 280 nm. We corrected the spectra by subtracting background spectra of samples of identical composition except that the protein was replaced with buffer.

Data Analysis. Experiments consisted of 3−7 trials with 10−14 titrations per trial. Trials were averaged point by point and then normalized individually. To obtain the partition coefficient (K_p) for membrane or tRNA binding, we used the changes in the CM of the intrinsic fluorescence spectra.

We note that although we use the term "K_p" throughout this paper, these values actually correspond to apparent partition coefficients since we assume that Gag partitions on membranes or RNA through nonspecific, electrostatic interactions rather than forming a chemical complex between a particular lipid(s) or nucleotide base(s).

$$K_p \text{ (i.e., } K_{app}) = ([P]_b/[L])/[P]_f$$

K_p is defined as the mole fraction of substrate-bound protein, $[P]_b/[L]$, divided by the concentration of free protein, $[P]_f$. $[P]_b$ is the concentration of substrate-bound protein, and [L] is the concentration of substrate. Each trial, as well as the average, was fit to a hyperbola using SigmaPlot (Jandel Inc.). The averaged data points, its associated K_p, and the fitted hyperbola are graphed. Errors were determined by

$$\text{error} = \text{ABS}\{(K_{p\,av} - K_{p\,x})/N\}$$

where the subscripts av and x and N denote the average K_p, the most different K_p of the individual trials, and the total number of trials, respectively.

The homotransfer studies monitored the self-association of Gag in solution, on membranes and on tRNA. Since the size of the Gag oligomers formed during the assembly pathway is unknown, we attempted to fit these data assuming Gag unimers aggregate to dimers, trimers, tetramers, or higher order species. We find that the best fit of the data assumes dimerization of Gag unimers, which have been reported to be trimers under many experimental conditions. On the basis of this analysis, we fit the fluorescence homotransfer data to a bimolecular association, and the dissociation constant, K_d, is reported.

Preparation of Cell Extracts. All plasmids were maintained in *Escherichia coli* strain C600. COS-1 cells were transfected by lipofection using the FuGene 6 transfection kit (Roche) according to the manufacturer's instructions. A DNA:FuGene 6 reagent ratio of 1:3 was used. Cells were incubated at 37 °C and 5% CO_2 for 48 h. After, transfected cells were scraped into media and collected by low-speed centrifugation. The pellet was washed twice with ice-cold PBS and resuspended in hypotonic buffer (10 mM Tris-HCl, pH 7.4, 0.2 mM $MgCl_2$). After 10−15 min on ice, the cells were disrupted by 30 strokes in a Dounce homogenizer with a tight-fitting type B pestle. Nuclei and unbroken cells were removed by centrifugation for 10 min at 1000*g*. The supernatant fraction was utilized as the cytoplasmic extract.

Sucrose Density Gradients. Sucrose solutions (20, 25, 30, 35, 40, 45, 50, 55, and 60%) in PBS (w/v) were prepared and filtered through 0.2 mm filters and stored at 4 °C. Then 111 mL of each, starting with the 60% solution, was layered in a centrifuge tube. The gradient was equilibrated for at least 3 h at 4 °C. After application of 300 mL of cytoplasmic extract, the gradient was centrifuged at 4 °C for 1 h at 50 000 rpm in a TLA 100 rotor, using a Beckman ultracentrifuge. Fractions (50 mL) were collected from the top of the tube, the density was measured with a refractometer, and the protein composition was determined by SDS−PAGE and immunoblotting.

SDS−PAGE and Western Blotting. Samples prepared for analysis on SDS−PAGE were mixed with an equal volume of 2× sample buffer, boiled for 3 min, and then loaded onto 12.5% SDS−polyacrylamide gels. Proteins separated on the basis of size by SDS−PAGE were transferred to nitrocellulose membranes with a Milliblot-Graphite Electroblotter II (Bio-Rad) according to the manufacturer's instructions.

Primary antibodies used were NEA-9306, a murine anti-HIV-1 CA monoclonal antibody (Dupont/NEN), and a rabbit anti-p6 polyclonal antibody (a generous gift of S. Campbell and A. Rein, NCI-FCRDC, Frederick, MD). The primary antibodies were detected by chemiluminescence (ECL-Amersham) using appropriate horseradish peroxidase-coupled secondary antibodies.

RESULTS

Binding of Gag Proteins to Membranes and tRNA. To differentiate the two possible assembly pathways (i.e., Gag first binds to membranes and then RNA, or vice versa), we measured and compared the changes in free energy of the individual steps. The changes in free energy of Gag binding to membrane or to tRNA were derived from the apparent partition coefficients (K_p) which were measured by the large decrease in fluorescence intensity (30−40%) of Gag as it binds to these negative surfaces as described in Materials and Methods (*16*). While the underlying molecular basis for this decrease has not been determined, it is presumed to be caused by quenching of Tyr/Trp fluorescence by the negative charges on the substrate surface.

We have previously characterized the ability of Gag to bind to large unilamellar vesicles of varying lipid compositions by fluorescence and sedimentation methods (*16*). Gag binds most strongly to negatively charged lipids, and since Gag is most soluble at high ionic strength (0.5 M NaCl), we measured its binding to large unilamellar vesicles composed of 1-palmitoyl-2-oleoyl-phosphatidylserine (POPS) prepared by extrusion in high-salt buffer. We find that the membrane binding ability of Gag_{WT} ($K_p = 5.2 \pm 0.4\ \mu M$) is twice as strong as that of $Gag_{\Delta MHR}$ ($K_p = 11.1 \pm 2.0\ \mu M$) (Figure 1A), in accord with previous studies (*15*). Since membrane binding is thought to be primarily through the N-terminal MA domain, this result implies that the MHR in the CA domain affects upstream protein conformation.

The same method was used to measure the reversible binding constant of Gag_{WT} and $Gag_{\Delta MHR}$ to tRNA. Interestingly, even though the MHR is thought to affect the conformation of the downstream C-terminal NC domain (*17*), the RNA binding ability of the mutant and wild types is approximately the same [$K_p = 4.0 \pm 0.1\ \mu M$ (base pair) and $K_p = 4.5 \pm 0.2\ \mu M$, respectively] (Figure 1B), leading to the conclusion that the MHR does not play a significant role in the association of Gag with RNA. We note that further studies (see below) indicate that Gag binds to these two substrates at distinct sites.

Self-Association of Membrane-Bound or RNA-Bound Gag Proteins. To monitor the self-association of Gag bound to substrate, we used both fluorescence heterotransfer and fluorescence homotransfer. Fluorescence heterotransfer refers to resonance energy transfer between two different probes whereas fluorescence homotransfer refers to energy transfer between identical fluorophores. In heterotransfer, one sample of protein is covalently labeled with a donor probe and another is labeled with an acceptor whose excitation spectrum overlaps the emission spectrum of the donor. Energy transfer

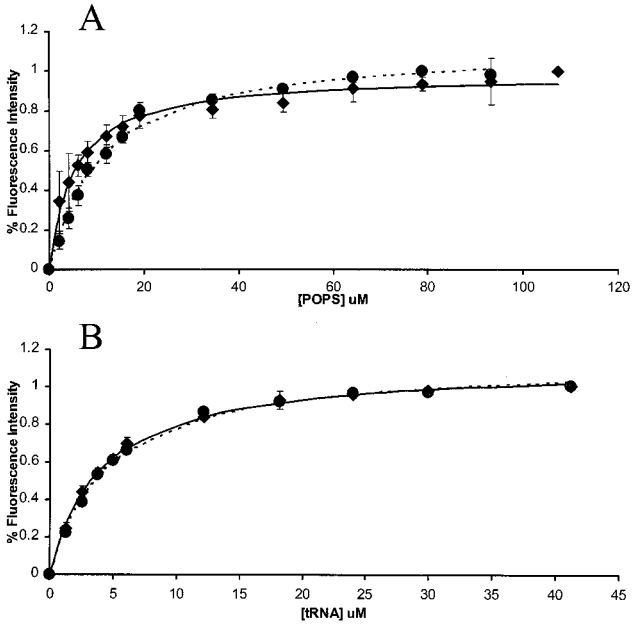

FIGURE 1: Binding of Gag proteins to lipid bilayers and RNA as followed by intrinsic tryptophan fluorescence. (A) Binding of 200 nM Gag_{WT} (◆) ($n = 5$) and 200 nM Gag_{MHR} (●) ($n = 3$) to POPS LUVs. (B) Binding of 200 nM proteins Gag_{WT} (◆) ($n = 4$) and $Gag_{\Delta MHR}$ (●) ($n = 3$) to tRNA.

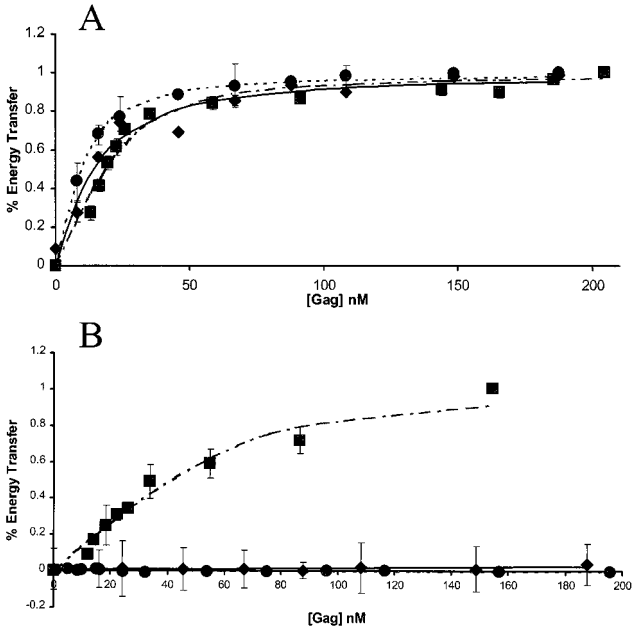

FIGURE 2: Self-association of Gag proteins on lipid bilayers and RNA where experimental data from fluorescence homotransfer and fluorescence heterotransfer were normalized and combined. (A) Gag_{WT} assembling into higher order oligomers on POPS LUVs (83 μM) (●) ($n = 3$), on tRNA (33 μM) (◆) ($n = 3$), and in buffer (■) ($n = 3$). (B) $Gag_{\Delta MHR}$ assembling into higher order oligomers on POPS (83 μM) (●) ($n = 10$), on tRNA (33 μM) (◆) ($n = 5$), and in buffer (■) ($n = 3$). $Gag_{\Delta MHR}$ energy transfer data on lipid and tRNA were normalized to Gag_{WT} homotransfer data on the same substrate.

will occur when the two probes come into close distance of each other and can be measured by the loss in donor emission or the gain in acceptor emission. In fluorescence homotransfer, the protein is covalently labeled with a probe whose emission spectrum overlaps with its absorption spectrum. If polarized light is used to excite the probes, then when the two probes are in energy transfer distance, the light will become depolarized. Protein assembly is then monitored by the loss in fluorescence anisotropy (see ref *18* for a more comprehensive description).

For the fluorescence heterotransfer studies, we labeled one set of the Gag proteins with the donor coumarin succinyl ester (CM) and another set with the nonfluorescence energy transfer acceptor dabsyl. Starting at a low concentration of CM−Gag (10 nM) either free in solution or bound to substrate, we then titrated dabsyl−Gag and measured the loss in coumarin fluorescence as compared to control solutions that contained only buffer. All samples showed an approximate 30% loss in donor fluorescence after correction for dilution.

For the fluorescence homotransfer studies, we labeled the Gag proteins with fluorescein at a 1:1 probe:protein ratio and monitored the decrease from an initial anisotropy of 0.088 ± 0.001 to 0.0233 ± 0.001 when incremental amounts of labeled protein are added as compared to the addition of buffer or unlabeled protein (both gave identical results). For simplicity, the resulting titration curves were then fit to a bimolecular dissociation constant (K_d), and the constants for Gag oligomerization in the presence and absence of binding substrates were compared (see Materials and Methods). We note that the fluorescein-labeled protein showed affinities identical to those of membranes and tRNA as unlabeled protein as determined in previous work (*16*) and in control studies.

In Figure 2A we show the assembly of Gag_{WT} in solution, on RNA, and on POPS bilayers where we normalized and combined the fluorescence homotransfer and fluorescence heterotransfer data. The dissociation constant of Gag in solution ($K_d = 18 \pm 1$ nM) is close to that obtained in the presence of excess tRNA ($K_d = 15 \pm 3$ nM) but somewhat weaker in the presence of excess membrane ($K_d = 9.5 \pm 1$ nM). This former result is explained by the observation that the tRNA molecules are small relative to Gag, and it is unlikely that more than one Gag could bind to a single tRNA. Hence, the tRNA−Gag complexes oligomerize similarly to unbound Gag presumably by contact sites that are distinct from the nucleic acid contact sites. On the basis of a reduction of dimensionality argument, we expected that the apparent affinity of membrane-bound Gag would be stronger than in solution. However, this concentrating effect is small since we choose experimental conditions so that Gag is always dilute on the bilayers and association can occur under conditions that mimic three-dimensional interaction. Presumably, if these self-association studies were done under conditions where the substrate would act to concentrate the Gag molecules on its surface, then the K_d values would be much lower (see ref *19*).

Identical studies were done using $Gag_{\Delta MHR}$. Interestingly, $Gag_{\Delta MHR}$ exhibits a much weaker self-association in buffer ($K_d = 42 \pm 6$ nM), clearly showing the importance of this region in protein oligomerization (Figure 2B). Strikingly, $Gag_{\Delta MHR}$ does not self-assemble on RNA or membranes in sharp contrast to the wild-type protein. This result clearly defines a critical role of the MHR in Gag assembly.

Secondary Binding of Bound Gag to the Second Substrate. We have found that membrane-bound Gag and tRNA-bound Gag undergo a further decrease in intrinsic fluorescence upon binding to the second substrate, which enabled us to use

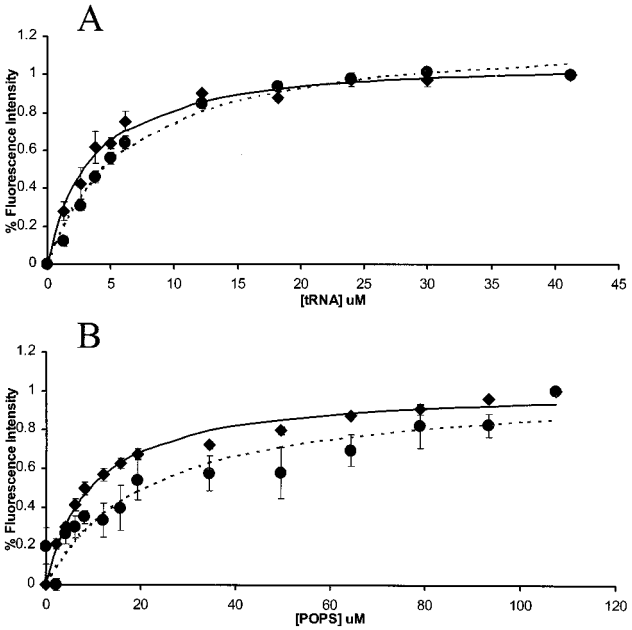

FIGURE 3: Binding of Gag−substrate complexes to lipid bilayers and RNA as followed by intrinsic tryptophan fluorescence. The complexes were formed using 200 nM protein and eight (40 μM) and then sixteen times (83 μM) the K_p of Gag_{WT} to POPS LUVs and four (16 μM) and then eight times (33 μM) the K_p of Gag_{WT} to tRNA. The concentrations of POPS LUVs and tRNA were based on the saturation curves seen in Figure 1. (A) Gag_{WT} (●) ($n = 3$) and $Gag_{\Delta MHR}$ (◆) ($n = 3$) complexed with POPS bound to tRNA. (B) Gag_{WT} (●) ($n = 3$) and $Gag_{\Delta MHR}$ (◆) ($n = 5$) complexed with tRNA bound to POPS.

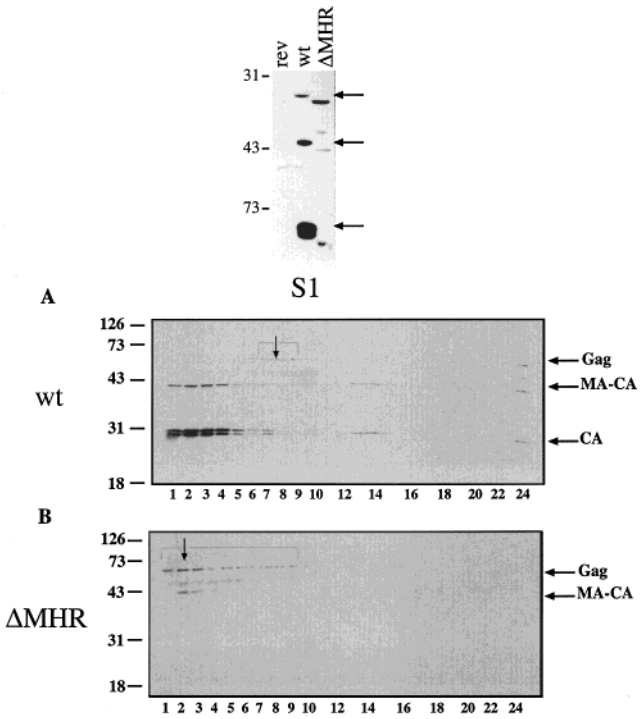

FIGURE 4: Sedimentation analysis of Gag assembly intermediates formed by Gag_{WT} and $Gag_{\Delta MHR}$. Cytoplasmic extracts prepared from COS-1 cells expressing Gag_{WT} or $Gag_{\Delta MHR}$ were layered on 20−60% sucrose gradients and centrifuged as described in Materials and Methods. Fractions were analyzed by SDS−PAGE and Western blotting using an antibody against the CA protein. Panels: A, GagWT; B, $Gag_{\Delta MHR}$. Molecular size markers are indicated on the left. The horizontal arrows on the right indicate the migration position of CA-related viral proteins. Brackets indicate fractions containing Gag. The vertical arrow indicates the peak fraction.

intrinsic fluorescence to measure the binding of membrane-bound Gag to tRNA and vice versa. The studies were done by preforming one of the complexes at substrate concentrations higher than the dissociation constant (i.e., 4- and 8-fold for tRNA and 8- and 16-fold for POPS) and titrating the second substrate into the cuvette. We find that POPS-bound Gag_{WT} binds to tRNA ($K_p = 3.4 \pm 0.4$ μM) more strongly than the $Gag_{\Delta MHR}$−POPS complex ($K_p = 6.3 \pm 0.1$ μM) (Figure 3A). Interestingly, the binding of Gag_{WT}−tRNA to POPS ($K_p = 9.6 \pm 0.9$ μM) is much stronger than that of $Gag_{\Delta MHR}$−tRNA ($K_p = 21.3 \pm 1.9$ μM) (Figure 3B). This reduced affinity is interpreted as being caused by the inability of MHR-deleted Gag to form productive complexes on tRNA.

Formation of Assembly Intermediates during Replication Requires the MHR. To determine whether the inability of $Gag_{\Delta MHR}$ to assemble on tRNA in solution also occurs in cells, we examined the effect of deleting the MHR on the formation of Gag assembly complexes in transfected mammalian cells.

HIV-1 Gag and Gag−Pol proteins were expressed in COS-1 cells using pgpRRE-r, a plasmid that expresses these proteins and Vif under the control of the SV40 late promoter. Expression of Gag and Gag−Pol from pgpRRE-r requires Rev, which was provided *in trans* by expression of the pCMV-rev plasmid. Rev allows the export of the unspliced gag and gag−pol mRNA out of the nucleus. pgpRRE-r encoding MHR-deleted Pr55Gag was constructed by removal of nucleotides 1184−1258 from the *gag* gene as previously described.

COS-1 cells were cotransfected with pCMV-rev and either pgpRRE-r or pgpRRE-r ΔMHR and harvested 48 h later. A cytoplasmic extract was prepared, and viral protein expression was checked by SDS−PAGE and Western blotting (Figure 4, inset). In the wild-type sample, an antibody against the CA domain in Gag recognized bands migrating at 55, 41, 25, and 24 kDa (lane 2) which correspond to the full-length Pr55Gag precursor, MA-CA (41 kDa) and CA-p2 (25 kDa) cleavage intermediates, and mature CA protein (24 kDa), respectively. These bands were not detected in cells transfected with pCMV-rev alone (lane 1). The sample expressing $Gag_{\Delta MHR}$ contained all of these proteins (lane 3). However, the proteins migrated slightly faster due to the 20 amino acid deletion, and there was relatively less proteolytic processing of the Pr55Gag precursor. This latter effect is interpreted as being due to the reduced membrane affinity of $Gag_{\Delta MHR}$ since processing occurs on the plasma membrane.

We assessed the distribution of assembly complexes of the cell lysates by velocity sedimentation on 20−60% sucrose density gradients, which separated the complexes by size and density. Fractions were collected from the gradients and analyzed by SDS−PAGE and immunoblotting using an antibody against the CA protein. In the wild-type sample (panel A), MA-CA, CA-p2, and CA were detected at the tip of the gradient in the position of soluble protein and in fractions 13−15 in the position of previously described immature particles ($r = 1.15$−1.17 g/mL). The uncleaved Pr55Gag precursor was detected in fractions 6−9, exhibiting the protein composition and density (1.08−1.11 g/mL) of previously described detergent-resistant replication com-

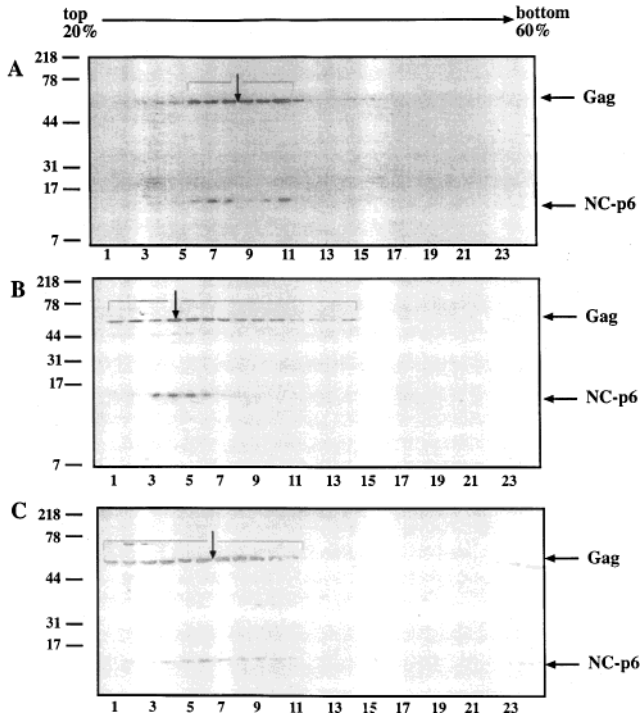

FIGURE 5: Characterization of the Gag assembly intermediate formed by Gag_{WT}. Aliquots of the cytoplasmic extract prepared from COS-1 cells expressing Gag_{WT} were incubated with RNase A or 1% IPEGAL prior to analysis on 20−60% sucrose gradients. The fractions were analyzed by SDS−PAGE and Western blotting using an antibody against the p6 protein. Panels: A, mock-treated extract; B, RNase A-treated extract; C, IPEGAL-treated extract. Molecular size markers are indicated on the left. The horizontal arrows on the right indicate the migration position of p6-related viral proteins. Brackets indicate fractions containing Gag. The vertical arrow indicates the peak fraction.

plexes (*20*). In contrast to the wild-type protein, most of the $Gag_{\Delta MHR}$ precursor accumulated as soluble protein at the top of the gradient ($r = 1.03-1.05$ g/mL; panel B) and clearly shows that the conformational state that drives productive processing is far less prevalent in the $Gag_{\Delta MHR}$ mutant.

The assembly complexes containing the unprocessed Pr55Gag precursor were further characterized by preincubating the lysate with RNase A (12 mg/mL), EDTA (20 mM), or the nonionic detergent IGEPAL (1%) for 1 h at 4 °C prior to layering on the sucrose gradient. A mock-treated sample was incubated under the same conditions with a comparable volume of buffer. The gradient fractions were analyzed by SDS−PAGE and immunoblotting using an antibody against the p6 protein in order to follow the RNA-binding NC-p1-p6 protein (Figure 5). The Pr55Gag precursor and NC-p1-p6 proteins in the mock-treated sample were detected in fractions 6−11 at a density of 1.08−1.12 (panel A). Treatment with RNase A shifted part of the Pr55Gag precursor and all of the NC-p1-p6 protein to fractions 4−6, the position of soluble proteins ($r = 1.04-1.06$ g/mL). A small amount of the Pr55Gag precursor also sedimented faster, suggesting that the original structure contained soluble proteins and immature particles in a complex that was stabilized by RNA. Treatment with the nonionic detergent did not significantly alter the migration of the Pr55Gag precursor or NC-p1-p6. The presence of a shift to lower densities upon RNase treatment to disrupt RNA−Gag complexes and the absence of a shift upon detergent treatment to disrupt lipid-Gag complexes imply that, in cells, RNA binding precedes membrane binding.

DISCUSSION

For infectious viral particle budding to occur, three essential components, the plasma membrane, viral RNA, and the structural precursor protein Gag, must associate. By comparison of the sequence of particle assembly of Gag_{WT} to $Gag_{\Delta MHR}$, the role of the MHR in this process may be assessed.

We first measured the binding affinity of Gag to lipid membranes and compared these values to the affinity for tRNA to determine the probable order of assembly in solution. We have expressed these affinities in units of micromolar lipid or micromolar base pair to make it easier to compare the affinities for the two substrates. Barring kinetic effects, if the binding of Gag to one of these substrates is much stronger than the other, this association would be expected to occur first. Here, we measured Gag binding to membranes and tRNA using intrinsic fluorescence. The validity of this method to accurately monitor substrate binding has been shown by sedimentation in the case of Gag−POPC association (*16*) and by mobility shifts in electrophoretic migration in native gels for Gag−RNA association (Goff et al., unpublished results). We conducted our measurements at elevated salt concentrations (0.5 M NaCl) because of the high propensity of Gag to aggregate at physiological ionic strengths. Thus, we can only evaluate the binding affinities at this salt level, and it is possible that reducing the ionic strength may affect their relative affinities. While the electrostatic component of membrane association of Gag can be determined simply by changing the headgroup composition (*16*), a similar determination for RNA binding is not as simple and is currently being investigated. Physiological conditions (i.e., reduced ionic strength and membrane surface charge) would favor RNA binding, which is consistent with the in vivo result obtained here.

Interestingly, the affinity of Gag for POPS and tRNA is very close, and the difference in free energy is within *RT* [600 cal/(mol·K)] (see Figure 6A and below). Thus, Gag would exhibit a preference for one substrate only if the other was limited. While it is possible that the affinity of Gag for native viral RNA is stronger than tRNA, which would make RNA the preferred substrate, in unpublished studies we did not detect significant differences in the energy of Gag binding to tRNA versus nonspecific mRNA or viral RNA on a base pair basis (Goff et al., unpublished results). The reproducible homogeneous composition of commercially available tRNA made its use preferable for these experiments.

Insight into the sequence of Gag assembly comes from sedimentation analysis of the Gag complex assembly in infected cells. These results suggest that initial Gag binding is to RNA due to the closer proximity of RNA to Gag as it is synthesized. Taken together, for Gag_{WT} our data support the assembly sequence in which Gag initially binds to RNA and self-associates, leaving the membrane binding face exposed for independent lipid interaction.

We have compiled our data in terms of a free energy diagram which allows us to assess whether binding of membrane-bound or tRNA-bound to the second substrate occurs with positive or negative cooperativity. Positive

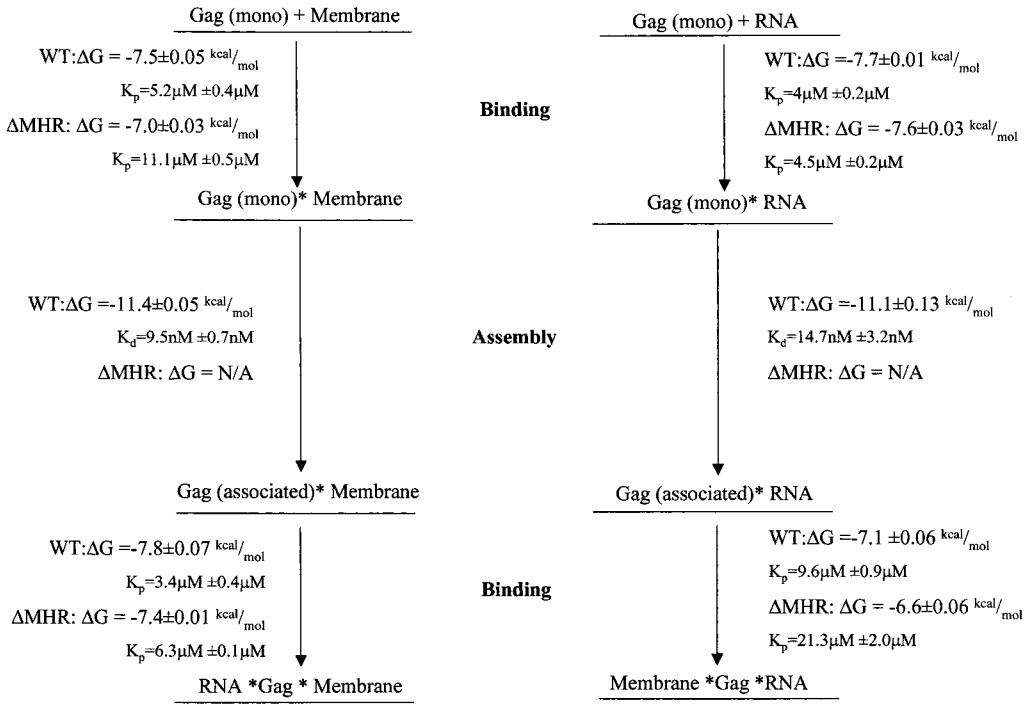

FIGURE 6: Free energy diagrams depicting the two possible pathways of particle formation. Free energy (ΔG) was calculated using $\Delta G = -RT \ln K$, with $R = 1.98722$ cal/(mol·K) and $T = 37$ °C. Errors in $\Delta G = RT$[(error in K)/K]. For Gag_{WT}, the total free energy change is -26.7 ± 0.2 kcal/mol for the first pathway and -25.9 ± 0.2 kcal/mol for the second pathway. For $Gag_{\Delta MHR}$, the sum of the two binding energies is -14.4 ± 0.1 kcal/mol for the first pathway and -14.2 ± 0.1 kcal/mol for the second pathway.

cooperativity would be expected if the binding of Gag to the first substrate resulted in an assemblage having a high local concentration of organized association sites that facilitated binding to the second substrate. Negative cooperativity would be expected if either the binding of Gag to the first substrate occluded the binding site for the second ligand, either directly or by an induced conformational change, or charge repulsion of the two negatively charged surfaces (POPC and tRNA) occurs. Cooperativity is indicated if the free energy change associated with binding of the complex to the target substrate differs from the free energy change associated with the free protein binding to the target substrate. From the data in Figure 6 we find that the ΔG for membrane association of Gag is similar (i.e., within *RT*) to the ΔG for the tRNA−Gag complex [−7.5 kcal/(mol·K) ∼ −7.8 kcal/(mol·K)]. Similarly, the ΔG for Gag association to tRNA is similar to the ΔG of the membrane−Gag complex [−7.7 kcal/(mol·K) ∼ −7.1 kcal/(mol·K)]. The observed lack of cooperativity leads to the conclusion that free Gag and substrate-associated Gag bind to the second substrate in a similar fashion and that charge repulsion plays a minor role. Possibly, neutralization by cationic Gag residues or higher ionic strength conditions that were used in these studies (0.5 M NaCl) minimized repulsion effects. We note that even though physiological ionic strength is lower than the one used here, which would increase charge repulsion between membrane and RNA, the inner leaflet of plasma membrane of cells is estimated to have ∼33% negatively charged lipids rather than the 100% used here (see ref *20*). On the basis of this argument and the results obtained here, charge repulsion is not expected to contribute under *in vivo* conditions.

The goal of this study was to gain insight into the energetic contribution of the MHR region in Gag assembly. This region is located in the central region of the CA domain of Gag, which in turn is located between the matrix and nucleocapsid domains. Thus, the MHR has the potential to affect both membrane and RNA interactions. MHR encompasses residues 153−172 of the CA domain of Gag, and inspection of the crystal structure (*22*) indicates that it forms an amphipathic helix. We have previously found that deletion and point mutations in the MHR weaken membrane binding (*15*), but it is unlikely that the MHR directly interacts with the membrane surface. More likely, the extensive network of hydrogen-bonding interactions between this region and other parts of the protein causes it to broadly influence Gag and CA conformation. This hypothesis is supported by observations that mutations within the MHR affect various steps during pre- and postassembly (*12*−*14*). This hypothesis is also supported by our finding that $Gag_{\Delta MHR}$ follows the same free energy pattern (Figure 6) as Gag_{WT} even though the membrane binding affinity of Gag_{WT} is stronger than that of $Gag_{\Delta MHR}$. Thus, it is likely that this deletion mutant follows the same order of assembly as wild type.

While $Gag_{\Delta MHR}$ has a somewhat impaired ability to self-associate in solution, the most striking difference between Gag_{WT} and $Gag_{\Delta MHR}$ was seen in the homotransfer experiments in the presence of membranes and tRNA. In sharp contrast to Gag_{WT}, when $Gag_{\Delta MHR}$ is bound to substrate, self-association is greatly inhibited. Thus, even though the contacts that $Gag_{\Delta MHR}$ makes with the membrane and tRNA are energetically on the same order as those of the wild type, the disposition of the protein on the surface leads to occlusion of the native protein−protein oligomerization sites either directly or through a conformational change, which in turns puts the proteins out of energy transfer range (i.e., ∼35 Å). This result leads to the conclusion that the MHR exhibits its largest effect on protein−protein interactions after substrate interaction. Together, these results suggest that $Gag_{\Delta MHR}$ first

binds to RNA but does not reveal the optimal membrane face relative of the wild type. Thus, the complex that binds to the membrane is expected to have altered protein−protein associations that result in disruption in the viral life cycle but not energetically altered membrane association sites. Work is underway to better understand these protein−protein associations.

ACKNOWLEDGMENT

We thank Indra Jayatilaka for technical assistance.

REFERENCES

1. Coffin, J. M., Hughes, S. H., and Varmus, H. E. (1997) *Retroviruses*, Cold Spring Harbor Laboratory Press, Plainview, NY.
2. Gelderbloom, H. R. (1991) *AIDS 5*, 617−638.
3. Facke, M., Janetzko, A., Shoeman, R. L., and Krausslich, H.-G. (1993) *J. Virol. 67*, 4972−4980.
4. Bukrinsky, M. I., Haggerty, S., Dempsey, M. P., Sharova, N., Adzhubei, A., Spitz, L., Lewis, P., Goldfarb, D., Emerman, M., and Stevenson, M. (1993) *Nature 365*, 666−669.
5. Luban, J., and Goff, S. P. (1991) *J. Virol. 65*, 3203−3212.
6. Aldorini, A., and Young, R. (1990) *J. Virol. 64*, 1920−1926.
7. Gorelick, R., Nigida, S., Bess, J., Arthur, L., Hendersen, L., and Rein, A. (1990) *J. Virol. 64*, 3207−3211.
8. Wills, J., and Craven, R. (1991) *AIDS 5*, 639−654.
9. von Poblotzki, A., Wagner, R., Niedrig, M., Wanner, G., Wolf, H., and Modrow, S. (1993) *Virology 193*, 981−985.
10. Franke, E. K., Yuan, H. E., and Luban, J. (1994) *Nature 372*, 359−362.
11. Gorelick, R., Hendersen, L., Hanser, J., and Rein, A. (1988) *Proc. Natl. Acad. Sci. U.S.A. 85*, 8450−8424.
12. Mammano, F., Ohagen, A., Hoglund, S., and Gottlinger, H. (1994) *J. Virol. 68*, 4927−4936.
13. Strambio de Castilla, C., and Hunter, E. (1992) *J. Virol. 66*, 7021−7032.
14. Craven, R., Leure-du-Pree, A., Weldon, R., and Wills, J. (1995) *J. Virol. 69*, 4212−4227.
15. Ebbets-Reed, D., Scarlata, S., and Carter, C. (1996) *Biochemistry 35*, 14268−14275.
16. Ehrlich, L., Fong, S., Scarlata, S., Zybarth, G., and Carter, C. (1996) *Biochemistry 35*, 3933−3943.
17. Boward, J. B., Bennett, R. P., Krishna, N., Ernst, S., Rein, A., and Wills, J. W. (1998) *J. Virol. 72*, 9034−9044.
18. Runnels, L., and Scarlata, S. (1995) *Biophys. J. 69*, 1569−1583.
19. Scarlata, S., Ehrlich, L. S., and Carter, C. A. (1998) *J. Mol. Biol. 277*, 161−169.
20. Lee, Y., Liu, B., and Yu, X. (1999) *J. Virol. 73*, 5654−5662.
21. Gennis, R. B. (1989) *Biomembranes: Molecular Structure and Function*, Springer-Verlag, New York.
22. Gamble, P., Yoo, S., Vajvos, F., von Schwedler, U., Worthphylake, D., Wang, H., McCutcheon, J., Sundquist, W., and Hill, C. (1997) *Science 278*, 849−853.

BI002040L